Advanced Energy Storage Management in Distribution Network

Guodong Liu*, Oğuzhan Ceylan†, Bailu Xiao*, Michael Starke*, Ben Ollis*, Daniel King*, Philip Irminger* and Kevin Tomsovic†
*Power and Energy Systems Group, Oak Ridge National Laboratory
Oak Ridge, Tennessee 37381
Email: liug@ornl.gov, xiaob@ornl.gov, starkemr@ornl.gov, ollistb@ornl.gov, kingdj@ornl.gov, irmingerp@ornl.gov
†Department of Electrical Engineering and Computer Science
University of Tennessee, Knoxville, Tennessee 37996
Email: oceylan@utk.edu, tomsovic@tennessee.edu

***Abstract*—With increasing penetration of distributed generation (DG) in the distribution networks (DN), the secure and optimal operation of DN has become an important concern. In this paper, an iterative mixed integer quadratic constrained quadratic programming model to optimize the operation of a three phase unbalanced distribution system with high penetration of Photovoltaic (PV) panels, DG and energy storage (ES) is developed. The proposed model minimizes not only the operating cost, including fuel cost and purchasing cost, but also voltage deviations and power loss. The optimization model is based on the linearized sensitivity coefficients between state variables (e.g., node voltages) and control variables (e.g., real and reactive power injections of DG and ES). To avoid slow convergence when close to the optimum, a golden search method is introduced to control the step size and accelerate the convergence. The proposed algorithm is demonstrated on modified IEEE 13 nodes test feeders with multiple PV panels, DG and ES. Numerical simulation results validate the proposed algorithm. Various scenarios of system configuration are studied and some critical findings are concluded.**

***Keywords*-Voltage regulation, sensitivity coefficients, linearization, distributed generation (DG), multiobjective optimization, unbalanced distribution network.**

NOMENCLATURE

The main symbols used in this paper are defined below. Others will be defined as required in the text. A symbol with $\triangle$ in front of it stand for the change of it. A symbol with (k) on the upper right position stands for its value of last iteration.

A. Indices and Numbers

i	Index of DGs, running from 1 to N_G.
e	Index of ESs, running from 1 to N_E.
j	Index of buses, running from 1 to N_J.
t	Index of time periods, running from 1 to N_T.
m	Index of energy blocks offered by DGs, running from 1 to N_I.

This work was sponsored by the Office of Electricity Delivery & Energy Reliability, U.S. Department of Energy under Contract No. DE-AC05-00OR 22725 with UT-Battelle and conducted at ORNL and UT Knoxville. This work also made use of Engineering Research Center Shared Facilities supported by the Engineering Research Center Program of the National Science Foundation and the Department of Energy under NSF Award Number EEC-1041877 and the CURENT Industry Partnership Program. The second author would like to thank the Scientific and Technological Research Council of Turkey (TUBITAK) for its financial support.

B. Variables

1) Binary Variables:

u_{it}	1 if DG i is scheduled on during period t and 0 otherwise.
u_{et}^{C}	1 if ES e is scheduled charging during period t and 0 otherwise.
u_{et}^{D}	1 if ES e is scheduled discharging during period t and 0 otherwise.

2) Continuous Variables:

$p_{it}\left(m\right)$	Power output scheduled from the m-th block of energy offer by DG i during period t. Limited to $p_i^{max}\left(m\right)$.
P_{it}	Real power output scheduled from DG i during period t.
Q_{it}	Reactive power output scheduled from DG i during period t.
P_{et}^{C}	Charging power of ES e during period t.
P_{et}^{D}	Discharging power of ES e during period t.
P_{et}	Net (discharging minus charging) power of ES e during period t.
SOC_{et}	State of charge of ES e during period t.
$\lvert V_{jt}\rvert$	Voltage magnitude of bus j during period t.
P_t^{In}	Purchased power from subtransmission grid during period t.
P_t^{Loss}	Total network power loss during period t.

C. Constants

$\lambda_{it}\left(m\right)$	Marginal cost of the m-th block of energy offer by DG i during period t.
$\lambda_t^{\mathrm{In}}\left(m\right)$	Purchasing price of energy from subtransmission grid during period t.
$P_i^{\max}$	Maximum output of DG i.
$P_i^{\min}$	Minimum output of DG i.
$P_e^{\mathrm{C,max}}$	Maximum charging power of ES e.

$P_e^{\mathrm{D,max}}$	Maximum discharging power of ES e.
$SOC_{et}^{\max}$	Maximum state of charge of ES e during period t.
$SOC_{et}^{\min}$	Minimum state of charge of ES e during period t.
η	ES efficiency factor.
A_i	Operating Cost of DG i at the point of P_i^{min}.
S_i	Apparent power limit of DG i.
S_e	Apparent power limit of ES e.
$tan(\theta)$	Power factor.

I. Introduction

With increasing penetration of distributed energy resources (e.g., wind turbines, PV panels, microturbines, fuel cells, mini-hydro, battery storage, and so on) in the distribution networks (DN), the traditional passive DNs without any generation sources are gradually transforming into active ones with both dispatchable and non-dispatchable generation sources in the following decades[1], [2]. Correspondingly, the usual "install and forget" principle will become infeasible as it could compromise operating efficiency. Within this context, new control and operation strategies capable of coordinating different types of distributed energy resources (DERs) efficiently to achieve operational objectives are in particular need of development [3].

Management and optimizing the operation of these active DNs require a full three-phase AC-formulation of the power flow equations, and various approaches have been proposed for solving the distribution optimal power flow (DOPF) problem in literature. Generally, these approaches can be classified into two categories. In the first category, the nonlinear optimization problem is directly solved using nonlinear programming methods such as gradient search or interior point methods [4]-[7]. It should be noted that the solution time and convergence characteristic of nonlinear programming in solving the DOPF problem may not satisfy the stringent time constraints required by real-time controls. In the second category, the nonlinear optimization problem is addressed by iteratively solving the linearized problem [8]-[13]. These linear programming based methods are generally more efficient in term of solution time. Nevertheless, the linearized problem is formulated based on the calculated sensitivity coefficients. When the solution is close to the optimum, the linearized sensitivities do not represent the nonlinear system correctly. In this case, the solution may hunt around the optimum and fail to converge.

Energy storage (ES) has been playing a more and more important role in the optimal operation of active distribution network and microgrids. By integrating ES into the operation of distribution network, various potential benefits can be gained, such as, active and reactive power flow control, demand charge reduction, compensation of renewable energy variation, power loss minimization, price arbitrage in energy market, voltage regulation, power factor correction, network congestion alleviation and intentional/unintentional islanding of portions of distribution network. To acquire these benefits, a optimal coordination among DG, ES, PV and possible demand response, as proposed in this paper, is necessary. It should be noted that DG in this paper means controllable distributed generation such as diesel generators, fuel cell, microturbines, etc. PV generation is traditionally controlled using maximum power point tracking (MPPT), which only depends on the weather condition. For this reason, PV is treated separately from DG. The optimal scheduling of ES in mocrogrids with high penetration of renewable energy sources has been studied in [14]-[16]. However, due to the limited generation capacity and the proximity of load and generation in a microgrid, the network model is not considered in the optimization model. To include the network model of distribution system, a multiobjective optimization problem that includes a three-phase unbalanced distribution network model is proposed and solved by Interior Point Optimizer (IPOPT) in [17]. A similar nonlinear programming model for optimal integration of ES in smart grid are solved by genetic algorithm in [18]. In order to handle the nonlinearity of distribution network model and improve the efficiency of optimization, an iterative linear or quadratic programming based method is proposed in [19]-[20]. To calculate the sensitivity coefficients more efficiently and accurately, a new linearization method of distribution network is proposed in [21], where various types of power injections (i.e. constant PQ, constant impedance and constant current) are taken into account and the accuracy of calculation is improved by removing the assumption of constant PQ injections.

This paper is a direct extension of [19] and [20] with improvements in multiple areas. An iterative mixed integer quadratic constrained quadratic programming model to optimize the operation of a three phase unbalanced distribution system is proposed. The model minimizes not only the operating cost, including fuel cost and purchasing cost, but also additional performance indices, including voltage deviations and power loss. The optimization model is based on the linearized sensitivity coefficients between state variables (e.g., node voltages) and control variables (e.g., real and reactive power injections of DG and ES). The proposed algorithm is demonstrated on the modified IEEE 13 nodes test feeders with multiple PVs, DGs and ESs. Numerical simulation results validate the proposed algorithm.

The main contributions of this paper are as follows.

1) A multiobjective optimization model is proposed to optimize both the economic and performance indices of the distribution network. The weighting coefficients of each objective are determined by using the analytical hierarchy process (AHP) [22].
2) To include the constraints of the startup and shutdown as well as the minimum output of DGs in the formulation of optimization, additional integer variables are

introduced. The power factor limits of DGs are also considered.

3) Various scenarios with different system configuration are studied. The necessity of unbalanced controllable sources for mitigating the imbalance of renewable resources and load in three-phase distribution network is demonstrated.

The rest of this paper is organized as follows. In Section II, the mixed integer quadratic constrained programming (MIQCP) formulation for multiobjective optimization problem is presented. In Section III, the proposed model is validated on modified IEEE 13 nodes test feeders. Various scenarios of system configuration are studied and some critical findings are identified. Section IV summarizes the paper and presents conclusions.

II. Methodology and Formulation

In this section, the MIQCP formulation for the optimal distribution of active DN is presented. The objective function and constraints are introduced separately. Then, an iterative optimization procedure with golden search method is illustrated.

A. Problem Definition

In the context of active DN, both dispatchable and undispatchable generation as well as ES are integrated into the network. The DN is also connected to an external subtransmission grid characterized by a given day-ahead hourly cost of energy exchange known for a time window of 24 hours. Under this assumption, the operation objective of active DN aims to minimize a virtual cost associated with the system operating cost and performance. The virtual cost includes: 1) cost of energy from DGs; 2) cost of purchasing energy from subtransmission grid; 3) voltage deviation; and 4) total network loss. The four objectives are combined into a single objective function by appropriate weighting. The objective function is

$$\begin{aligned}\min_{\triangle \mathrm{x}} \quad & W_F \left\{ \sum_{t=1}^{N_T} \sum_{i=1}^{N_G} \left[\sum_{m=1}^{N_I} \lambda_{it}(m) p_{it}(m) + A_i u_{it} \right] \right. \\ & \left. + \sum_{t=1}^{N_T} \sum_{i=1}^{N_G} S_{it}\left(u_{it}, u_{i,t-1}\right) \right\} \\ & + W_P \left(\sum_{t=1}^{N_T} \lambda_t^{In} P_t^{In} \right) \\ & + W_V \left[\sum_{t=1}^{N_T} \sum_{j=1}^{N_J} \left(|V_{jt}| - 1 \right)^2 \right] \\ & + W_L \left(\sum_{t=1}^{N_T} P_t^{Loss} \right) \end{aligned} \tag{1}$$

where $\triangle x = [\triangle P_{it}, \triangle Q_{it}, \triangle P_{et}, \triangle Q_{et}]$ is the control variable vector, $\triangle x = \left[\triangle P^{DER}, \triangle Q^{DER}\right]$ is the control variable vector, N_G is the number of DERs and N_B is the number of nodes. Specifically, the first and second line is the energy cost of DGs (including DG start-up cost); the third line is the energy purchasing cost from subtransmission grid; the fourth line is the voltage deviation; and the last line is the total network loss. It should be noted that the voltage magnitude is in per-unit form, thus the target of voltage magnitude is 1 as shown in the fourth line of (1). All terms are in mixed-integer linear or quadratic form except the startup cost of DGs, which can be recast into mixed-integer linear form as in [23]. The weighting coefficients W_F, W_P, W_V and W_L can be determined by using the analytical hierarchy process (AHP) [22]. First of all, a pairwise comparison is done between the objectives. By this way, the relative importance of each factor in comparison with all other factors will be defined by the decision-maker, who may have difference preferences from network to network. Then, a matrix is built based on these comparisons. Finally, the weighting coefficients are calculated based on the matrix.

B. Constraints

The objective function must be minimized subject to a number of constraints. For simplicity, these constraints are grouped into constraints of DGs, constraints of ESs and network constraints.

1) Constraints of DG: It should be noted that DGs are assumed to be three-phase balanced sources. The constraints associated with DGs include the following:

$$P_{it} = \sum_{m=1}^{N_I} p_{it}(m) + u_{it} P_i^{\min} \quad \forall i, \forall t \tag{2}$$

$$0 \le p_{it}(m) \le p_i^{\max}(m) \quad \forall i, \forall t, \forall m \tag{3}$$

$$P_{it} \le P_i^{max} u_{it} \quad \forall i, \forall t \tag{4}$$

$$\sum_{m=1}^{N_I} p_i^{max}(m) + P_i^{\min} = P_i^{max} \quad \forall i, \forall t \tag{5}$$

$$-tan(\theta) P_{it} \le Q_{it} \le tan(\theta) P_{it} \quad \forall i, \forall t, \forall p, \forall w \tag{6}$$

$$\left(P_{it}\right)^2 + \left(Q_{it}\right)^2 \le S_i^2 \quad \forall i, \forall t \tag{7}$$

$$p_{it}(m) = p_{it}^{(k)}(m) + \triangle p_{it}(m) \quad \forall i, \forall t, \forall m \tag{8}$$

$$Q_{it} = Q_{it}^{(k)} + \triangle Q_{it} \quad \forall i, \forall t \tag{9}$$

$$P_{it} = P_{it}^{(k)} + \triangle P_{it} \quad \forall i, \forall t \tag{10}$$

Constraints (2) and (3) approximate the energy cost of DGs by blocks and (4) enforces the output of DG to be zero if it is not committed. The power factor and capacity limit is ensured by (6) and (7). Since the optimization problem takes advantage of the sensitivity coefficients calculated by linearizing the system under the operating point of last

iteration, the control variables are actually the deviations of active and reactive power of DGs and ES from their current operating points. This relationship is ensured by (8) - (10).

2) Constraints of Energy Storage: ESs are assumed to be three-phase unbalanced sources here, but the three-phase charging/discharging power can be easily enforced to be equal by adding additional equality constraints. The constraints associated with ESs include the following:

$$0 \le P_{et}^{\mathrm{C}} \le P_{e}^{\mathrm{C,max}} u_{et}^{\mathrm{C}} \quad \forall e, \forall t \tag{11}$$

$$0 \le P_{et}^{\mathrm{D}} \le P_{e}^{\mathrm{D,max}} u_{et}^{\mathrm{D}} \quad \forall e, \forall t \tag{12}$$

$$u_{et}^{\mathrm{C}} + u_{et}^{\mathrm{D}} \le 1 \quad \forall e, \forall t \tag{13}$$

$$SOC_{et} = SOC_{e,t-1} + P_{et}^{\mathrm{C}}\eta - P_{et}^{\mathrm{D}}\frac{1}{\eta} \quad \forall e, \forall t \tag{14}$$

$$SOC_{et}^{\min} \le SOC_{et} \le SOC_{et}^{\max} \quad \forall e, \forall t \tag{15}$$

$$P_{et} = P_{et}^{D} - P_{et}^{C} \quad \forall e, \forall t \tag{16}$$

$$\left(P_{et}\right)^2 + \left(Q_{et}\right)^2 \le S_e^2 \quad \forall e, \forall t \tag{17}$$

$$P_{et}^{\mathrm{C}} = P_{et}^{C,(k)} + \triangle P_{et}^{\mathrm{C}} \quad \forall e, \forall t \tag{18}$$

$$P_{et}^{\mathrm{D}} = P_{et}^{D,(k)} + \triangle P_{et}^{D} \quad \forall e, \forall t \tag{19}$$

$$Q_{et} = Q_{et}^{(k)} + \triangle Q_{et} \quad \forall e, \forall t \tag{20}$$

$$\triangle P_{et} = \triangle P_{et}^{D} - \triangle P_{et}^{C} \quad \forall e, \forall t \tag{21}$$

Constraint (11) and (12) are the maximum charging/discharging power of ESs. These two states are mutually exclusive, which is ensured by (13). The state of charge (SOC) limits are enforced by (14) and (15). The net power (discharging minus charging) of ESs is represented by (16) and the capacity limit id ensured by (17) . Similar to constraints of DGs, the control variables are the deviations for active and reactive power of ESs, which is ensured by (18) - (21).

3) Network Constraints: In this paper, a three-phase unbalanced DN is taken into account. The voltage magnitudes of each phase at each node are constrained by (22). The state variables are represented as the sum of its values in the previous iteration and the changes in the current iteration as in (22) - (25). In (26) - (28), the changes of state variables (voltage magnitude, purchased power and network loss) are expressed as a linear function of the changes of control variables (real and reactive power of DGs and ESs). In particular, K_{jit}^{P} and K_{jit}^{Q} are the sensitivity of real and reactive power output of DG i at time t to the voltage magnitude of bus j; H_{it}^{P} and H_{it}^{Q} are the sensitivity of real and reactive power output of DG i at time t to the total purchasing power at time t; and L_{it}^{P} and L_{it}^{Q} are the sensitivity of real and reactive power output of DG i at time t to the total network loss at time t. The calculation of these sensitivity coefficients is based on the method in [21] due to its efficiency and accuracy.

$$0.95 \le |V_{jt}| \le 1.05 \quad \forall j, \forall t \tag{22}$$

$$|V_{jt}| = |V_{jt}|^{(k)} + \triangle |V_{jt}| \quad \forall j, \forall t \tag{23}$$

$$P_t^{In} = P_t^{In,(k)} + \triangle P_t^{In} \quad \forall t \tag{24}$$

$$P_t^{Loss} = P_t^{Loss,(k)} + \triangle P_t^{Loss} \quad \forall t \tag{25}$$

$$\begin{aligned} \triangle |V_{jt}| \;=\; & \sum_{i=1}^{3N_G} \left(K_{jit}^{P} \triangle P_{it} + K_{jit}^{Q} \triangle Q_{it} \right) \\ & + \sum_{e=1}^{N_E} \left(K_{jet}^{P} \triangle P_{et} + K_{jet}^{Q} \triangle Q_{et} \right) \forall j, t \end{aligned} \tag{26}$$

$$\begin{aligned} \triangle P_t^{In} \;=\; & \sum_{i=1}^{3N_G} \left(H_{it}^{P} \triangle P_{it} + H_{it}^{Q} \triangle Q_{it} \right) \\ & + \sum_{e=1}^{N_E} \left(H_{et}^{P} \triangle P_{et} + H_{et}^{Q} \triangle Q_{et} \right) \quad \forall t \end{aligned} \tag{27}$$

$$\begin{aligned} \triangle P_t^{Loss} \;=\; & \sum_{i=1}^{3N_G} \left(L_{it}^{P} \triangle P_{it} + L_{it}^{Q} \triangle Q_{it} \right) \\ & + \sum_{e=1}^{N_E} \left(L_{et}^{Q} \triangle P_{et} + L_{et}^{Q} \triangle Q_{et} \right) \quad \forall t \end{aligned} \tag{28}$$

C. Iterative Optimization Procedure with Golden Search Method

The formulated optimization problem (1-28) is then solved by means of a MIQP algorithm in order to find the improvement direction $\triangle x$ of the control variable vector $x = [P_{it}, Q_{it}, P_{et}, Q_{et}]$. For each iteration, the current values of the control variables are modified by $\triangle x$ and the new direction is calculated based on the updated sensitivity coefficients at current operating condition. This iterative procedure continues until the objective function or the control variables do not change significantly between two consecutive iterations or a maximum number of iterations is reached. In addition, a nonlinear one dimensional optimization problem is solved by the golden search method to determine the optimal step size ξ of the control variables when an oscillation is detected [8], [20]. Then, the improvement direction $\triangle x^{(k+1)}$ is modified by $\xi \triangle x^{(k+1)}$. In this way, the hunting around the solution is avoided and convergence accelerates. The iterative optimization procedure with golden search method is shown is Fig. 1.

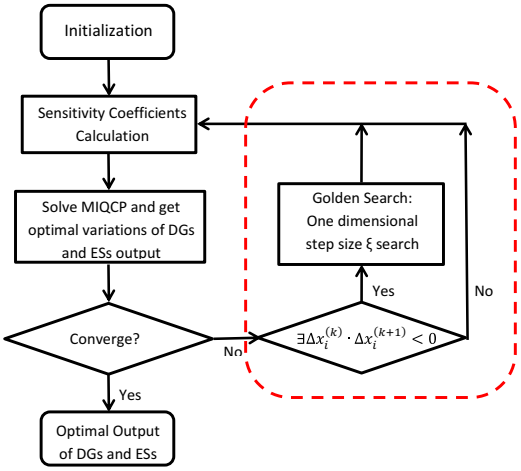

Figure 1: Iterative optimization procedure with golden search method

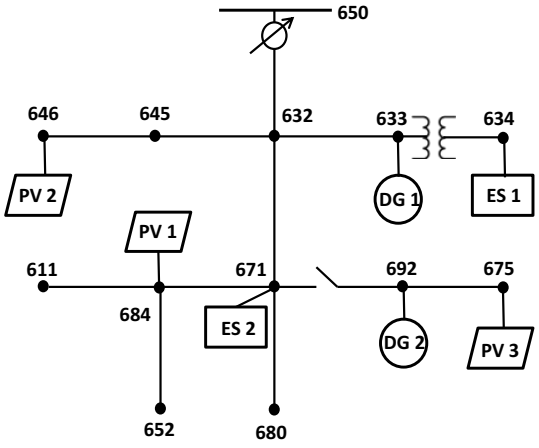

Figure 2: Modified IEEE 13 nodes test feeder

III. Case Studies

A. Test System Data

The proposed iterative optimization procedure is demonstrated on a modified IEEE 13 nodes test feeder as shown in Fig. 2 [24]. All together 3 PVs, 2 DGs and 2 ESs were added to the system. The location, phase and capacity information is shown in Table I. The DGs are assumed to be have three phase balanced output, while the ESs are assumed to be three-phase unbalanced sources here, but the three-phase charging/discharging power can be easily enforced to be equal by adding additional equality constraints.

The analysis is conducted for a 24-hour scheduling horizon and each time interval is set to be one hour. The load profile for the 24 hours is obtained by scaling the original load data. The scaling factors are calculated based on the load profile in [25] and shown in II. The load types (e.g., constant power, constant impedance and constant current) are not changed. The day-ahead market price of subtransmission grid is also shown in II. The parameters for the DGs are shown in Table III. For simplicity, the quadratic cost curves are converted into three-piece piece-wise linear cost curves. Minimum up and down time as well as the ramping rates are neglected.

The PV model is from [26]. The solar irradiance and temperature data is measured data from [27]. The battery efficiency is assumed to be 0.9. All numerical simulations are coded in MATLAB and solved using the MIQP solver CPLEX 12.2. With a pre-specified duality gap of 0.1%, the running time of each case is about 90 seconds on a 2.66 GHz Windows-based PC with 4 G bytes of RAM.

Table I: PVs, DGs, and ESs added to the IEEE 13 Node Test Feeder

Bus No.	Component	Phases	Capacity
684	PV	a and c	300 kW (per phase)
646	PV	b and c	300 kW (per phase)
675	PV	a, b and c	300 kW (per phase)
633	DG	a, b and c	360 kW (three-phase total)
692	DG	a, b and c	180 kW (three-phase total)
634	ES	a, b and c	100kW/200kWh (per phase)
671	ES	a, b and c	100kW/200kWh (per phase)

Table II: Load scaling factors and day-ahead market prices

Hour	Load Scaling Factor	Price (ct/kWh)	Hour	Load Scaling Factor	Price (ct/kWh)
1	0.7640	8.65	13	1.1640	26.82
2	0.7596	8.11	14	1.1461	27.35
3	0.7775	8.25	15	1.1775	13.81
4	0.7640	8.10	16	1.1910	17.31
5	0.7865	8.14	17	1.1461	16.42
6	0.8315	8.13	18	1.1371	9.83
7	0.8989	8.34	19	1.1236	8.63
8	1.0921	9.35	20	1.1461	8.87
9	1.1416	12.0	21	1.1685	8.35
10	1.1685	9.19	22	1.1146	16.44
11	1.2000	12.3	23	0.9888	16.19
12	1.1640	20.7	24	0.8270	8.87

B. Effect of Weighting Factors

As mentioned above, the weighting coefficients of each term in the objective function are determined by using AHP.

Table III: Parameters of DGs

Unit Type	Min. Power (kW)	Max. Power (kW)	Startup Cost ($)	Operating Cost ($) $(a + bP + cP^2)$		
				a	b	c
Diesel (DG 1)	90	360	6	0.6500	0.0152	0.00052
Microturbine (DG 2)	60	180	3	0.2000	0.0198	0.00026

Table IV: Evaluation of solutions of single objective optimization and multiobjective optimization

	Single Objective Optimization Solutions				Multiobjective Optimization Solution
	Optimizing Voltage	Optimizing Loss	Optimizing Fuel Cost	Optimizing Purchasing Cost	
Voltage Deviation (pu)	0.4506	0.8468	0.8188	0.9989	0.8066
Loss (kW)	2277.04	1705.93	2213.45	2017.70	2027.88
Fuel Cost ($)	907.06	2257.53	62.41	2269.21	302.99
Purchasing Cost ($)	10411.34	9523.48	11149.92	9271.99	10392.18

Table V: Pairwise comparisons of the objective terms

	Fuel Cost of DGs	Purchasing Cost	Voltage Deviation	Network Loss
Fuel Cost of DGs	1	2	1/3	3
Purchasing Cost	1/2	1	1/5	2
Voltage Deviation	3	5	1	10
Network Loss	1/3	1/2	1/10	1

Table VI: Voltage deviations with different weighting coefficients

Cases	Base case	Base case with $W_V \times 100$	Single objective case
Voltage Deviation (pu)	0.8066	0.5282	0.4506

The pairwise comparisons of these terms are shown in Table V. This pairwise comparison matrix is fed into the AHP and the weighting coefficients of each term are calculated as: W_F=0.2084, W_P=0.1171, W_V=0.6116, and W_L=0.0629. It should be noted that the system operator can change the pairwise comparison matrix according to the system configuration and their preference.

In order to show the benefit of multiobjective optimization, both single objective optimization problems and multiobjective optimization problem are solved. The solutions, i.e., real and reactive power of DGs and ESs are evaluated by calculating the corresponding terms, i.e., voltage deviation, total network loss, fuel cost and purchasing cost. The results are shown in Table IV. As can be seen, when the problem is formulated as a single objective optimization, the targeted terms are always optimized to the best (as shown in red) compared to that of other solutions (the rest in the same row). By multiobjective optimization, none of these terms are their optimal, but a comprise is reached among all terms. Specifically, the new solution for voltage deviation and fuel cost are second best among the listed solutions; while network loss and purchasing cost are third best among the available solutions. This is because the weighting coefficients of voltage deviation (W_F) and fuel cost (W_F) are much larger than those of purchasing cost (W_P) and network loss (W_L). Nevertheless, all of these solutions are Pareto optimal, i.e., one cannot improve one term without sacrificing another.

To show the effect of weighting coefficients, the distribution density of voltages corresponding to all nodes for the whole period is shown in Fig. 3 In particular, 3a refers to the base multiobjective case in Table IV; 3b refers to the base case with W_V multiplied by 100, which means the distribution system operator prefers better voltage profiles than other terms, whilst 3c refers to the single objective optimization minimizing only voltage deviation. As can be seen, as the weighting coefficient W_F becomes bigger, the distribution of voltages gets closer to 1 p.u. and the fat tails are reduced, which means the voltage profiles are getting better. Particularly, the voltage profiles are significantly improved by single objective optimization, which only optimizes the voltage deviations. The voltage diviations for these three cases are calculated and shown in Table VI. It shows clearly that the voltage deviation decreases when the weighting coefficient on voltage deviation increases.

C. Real Power Coordination of DGs, ESs and Subtransmission Grid

The relationship between day-ahead market price and real power output of DGs and ES 1 solved by the base multiobjective case is shown in 4. ES 1 at node 634, includes three batteries, battery 1 is connected to phase A; battery 2 is connected to phase B; and battery 3 is connected to phase C. These three batteries are operated independently. When the market price is high, both DG1 and DG 2 increase power output and all batteries discharge real power. Correspondingly, when the market price is low, DGs decrease power output and batteries charge.

D. Reactive Power of DGs and ESs

The relationship between voltage at node 634 phase A and reactive power output of battery 1 in ES 1 and battery 4 in ES2 solved by the base multiobjective case as shown in 5. ES 2 at node 671 include three batteries, battery 4 is connected to phase A; battery 5 is connected to phase B; and battery 6 is connected to phase C. So, both battery 1 and 4 are connected to phase A. As can be seen, both batteries generate reactive power to support the voltage at node 634 phase A. In addition, battery 1 is more sensitive than battery 4, this is because battery 1 is closer to node 634 than battery 4.

E. Effect of Different System Configurations

In order to identify the importance of resources with three-phase independent output, we constructed three additional

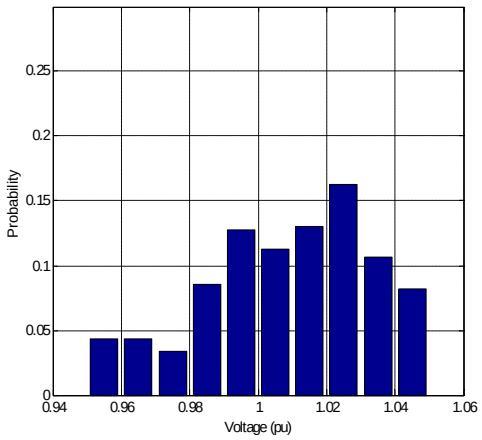

(a) Base case (multiobjective optimization)

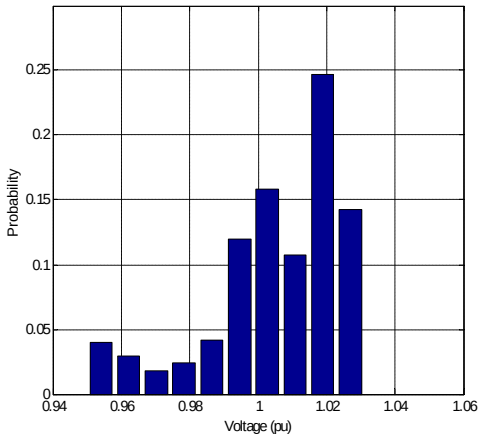

(b) Base case with $W_V \times 100$

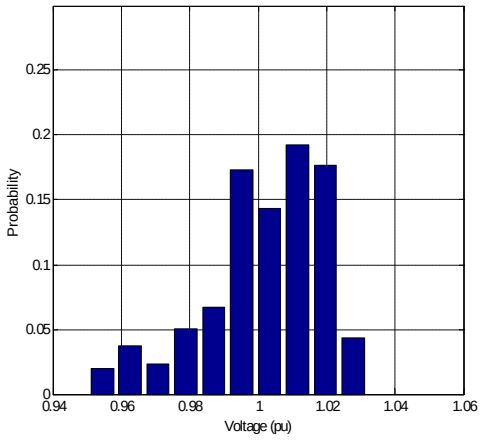

(c) Single objective case (only minimizing voltage deviations)

Figure 3: Distribution density of voltages for all nodes and all periods

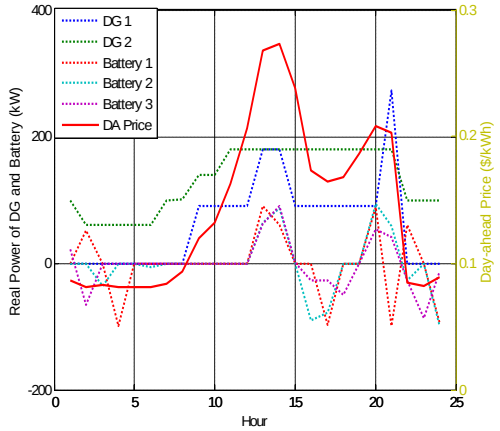

Figure 4: Day-ahead market price and real power output of DGs and ESs

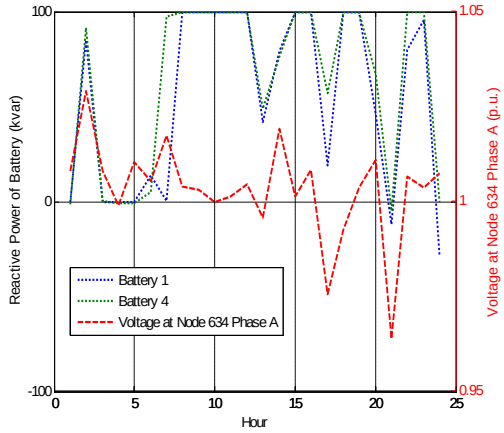

Figure 5: Voltage at Node 634 phase A and reactive power output of battery 1and 4

scenarios with different system configurations. Scenario 1 only has PV integrated and all DGs and ESs are disabled; scenario2 has PV and DGs with three-phase balanced output; scenario 3 has PVs, DGs and ESs, but the ESs are enforced to be three-phase balanced sources by adding additional constraints; and scenario 4 is the base multiobjective case in Table IV. Fig. 6a shows significant overvoltage and undervoltage issues arise when large scale unbalanced PV is integrated. In Fig. 6b, the voltage issues cannot be eliminated by adding three-phase balanced DGs, which indicates the imbalance of voltages among three phases. In 6c adding three-phase balanced ESs cannot improve the voltage profile either. Finally, by adding ESs with three-phase independent output, the voltage profiles are significantly improved as shown in Fig. 3a. To be more clear, the voltage diviations for these four scenarios are calculated and shown in Table VII. As can be seen, the voltage deviation increases when more

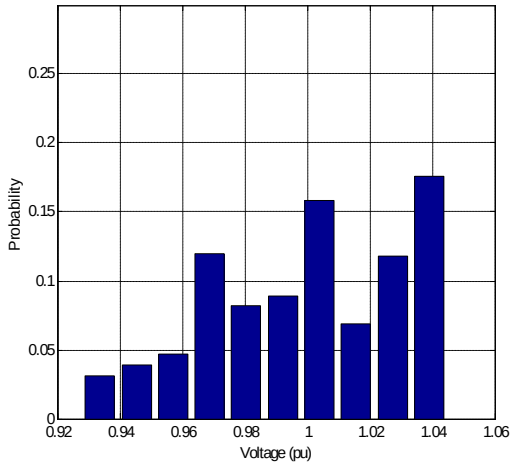

(a) Scenario 1: PV only

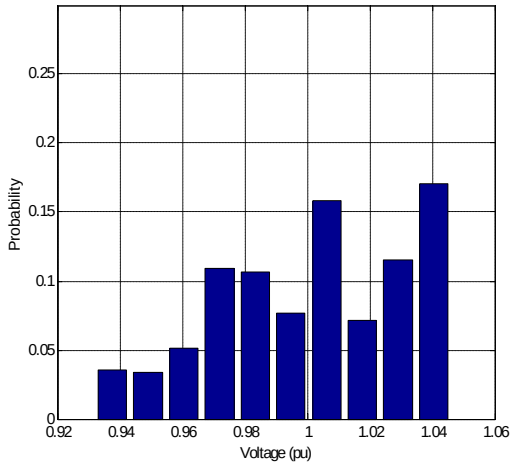

(b) Scenario 2: PV and DGs

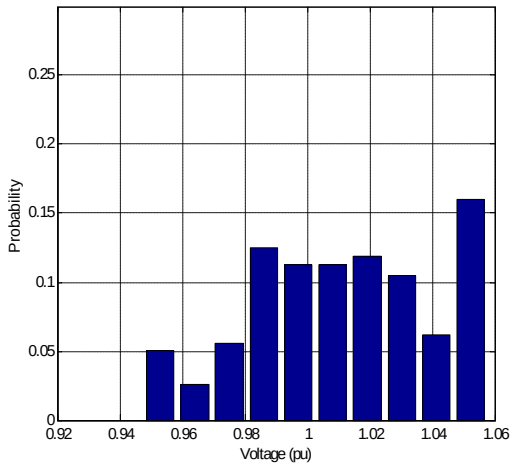

(c) Scenario 3: PV, DGs and balanced ESs

Figure 6: Distribution density of voltages for scenarios with different system configurations

Table VII: Voltage deviations with different system configurations

Cases	Scenario 1: Only PV	Scenatio 2: PV and DG	Scenatio 3: PV, DG and phase balanced ESs	Scenatio 4: PV, DG and phase independent ESs
Voltage Deviation (pu)	0.9684	1.0125	1.0494	0.8066

phase balanced resources such as DG and ES are integrated into the system, while significantly decreases when phase independent ESs are added. This means that to eliminate the imbalance of voltages in this three-phase unbalanced distribution network, it is necessary to have controllable sources with three-phase independent output capability.

IV. Conclusions

In this paper, an iterative MIQCP model to optimize the operation of a three phase unbalanced distribution system with high penetration of PV, DG and energy storage (ES) is proposed. Four objectives including fuel cost, purchasing cost, voltage deviations and network power loss are combined into a single objective function by assigning weighting coefficients, which are determined by AHP. Numerical simulations on a modified IEEE 13 nodes test feeder show the effectiveness of the proposed model. The benefits of multiobjective optimization are demonstrated and the effects of weighting coefficients are validated. In addition, the necessity of unbalanced controllable sources for mitigating the imbalance of renewable resources and load in three-phase distribution network is demonstrated.

Noted that the uncertainty associated with renewable DG is not considered in this paper. However, the optimization model proposed in this paper can be easily extended into a two-stage stochastic optimization model, in which uncertainty of renewable will be considered as various scenarios and compensated by the battery charging/discharging power for each scenario in the lower stage. The startup and shutdown decision of DG as well as the battery charging/discharging decision will be decided in the higher stage and kept the same across all scenarios in the lower stage. To handle the dimensionality issue with large systems, scenario reduction technique can be used to reduce the number of scenarios while preserves the credibility of the reduced scenario set [28]. Case studies on larger systems considering uncertainty associated with renewable DG will be studied in the future work.

References

[1] J. A. P. Lopes, N. Hatziargyriou, J. Mutale, P. Djapic, and N. Jenkins, "Integrating distributed generation into electric power systems: A review of drivers, challenges and opportunities," *Elect. Power Syst. Res.*, vol. 77, no. 9, pp. 1189–1203, 2007.

[2] Navigant Research, “Global Distributed Generation Deployment Forecast : Solar PV, Small Wind, Fuel Cell, Natural Gas Generator Set, and Diesel Generator Set Capacity and Revenue by Country and Technology: 2014-2023,” Aug. 2014.

[3] Y. Zhu and K. Tomsovic, “Optimal Distribution Power Flow for Systems with Distributed Energy Resources,” *Int. J. Elect. Power Energy Syst.,* vol. 29, no. 3, pp. 260-267, Mar. 2007.

[4] S. Gill, I. Kockar and G.W. Ault, “Dynamic Optimal Power Flow for Active Distribution Networks,” *IEEE Trans. Power Syst.*, vol. 29, no. 1, pp. 121-131, Jan. 2014

[5] .N. Daratha, B. Das and J. Sharma, “Coordination Between OLTC and SVC for Voltage Regulation in Unbalanced Distribution System Distributed Generation,” *IEEE Trans. Power Syst.* , vol. 29, no. 1, pp. 289-299, Jan. 2014.

[6] M. J. Dolan, E. M. Davidson, I. Kockar,G.W. Ault and S. D. J. McArthur, “Distribution Power Flow Management Utilizing an Online Optimal Power Flow Technique,” *IEEE Trans. Power Syst.* vol. 27, no. 2, pp. 790-799, May 2012.

[7] S. Paudyal,C. A. Canizares and K. Bhattacharya, “Optimal Operation of Distribution Feeders in Smart Grids,” *IEEE Trans. Ind. Electron.*, vol. 58, no. 10, pp. 4495-4503, Oct. 2011.

[8] A. Borghetti, M. Bosetti, S. Grillo, S.Massucco, C. Nucci,M. Paolone, and F. Silvestro, “Short-term scheduling and control of active distribution systems with high penetration of renewable resources,” *IEEE Syst. J.*, vol. 4, no. 3, pp. 313–322, Sep. 2010.

[9] Q. Zhou and J. Bialek, “Generation curtailment to manage voltage constraints in distribution networks,” *IET Gener., Transm., Distrib.*, vol. 1, no. 3, pp. 492–498, May 2007.

[10] V. Calderaro, G. Conio, V. Galdi, G. Massa and A. Piccolo, “Optimal Decentralized Voltage Control for Distribution Systems With Inverter-Based Distributed Generators,” *IEEE Trans. Power Syst.,* vol. 29, no. 1, pp. 230-241, Jan. 2014.

[11] A. Borghetti, M. Bosetti, S. Grillo, M. Paolone, and F. Silvestro, “Short-Term Scheduling of Active Distribution Systems,” in *Proc. 2009 IEEE Power Tech Conf.*, Bucharest, Romania, Jun.28–Jul. 3 2009.

[12] A. Keane and M. O’Malley, “Optimal Allocation of Embedded Generation on Distribution Networks,” *IEEE Trans. Power Syst.*, vol. 20, no. 3, pp. 1640-1646, Aug. 2005.

[13] Y. P. Agalgaonkar, B.C. Pal and R.A. Jabr, “Distribution Voltage Control Considering the Impact of PV Generation on Tap Changers and Autonomous Regulators,” *IEEE Trans. Power Syst.,* vol. 29, no. 1, pp. 182-192, Jan. 2014.

[14] R. Rigo-Mariani, B. Sareni, and X. Roboam, “A fast optimization strategy for power dispatching in a microgrid with storage,” in *Proc. 2013 IEEE Industrial Electronics Society, IECON 2013*, pp.7902-7907, Nov. 10-13, 2013

[15] D. Wang, S. Ge, H. Jia, C. Wang, Y. Zhou, N. Lu, and X. Kong, “ A demand response and battery storage coordination algorithm for providing microgrid tie-line smoothing services," *IEEE Trans. Sustain. Energy*, vol. 5, no. 2, pp. 476-486, Apr. 2014.

[16] B. Zhao, Y. Shi, X. Dong, W. Luan, and J. Bornemann, “Short-term operation scheduling in renewable-powered microgrids: A duality-based approach,” *IEEE Trans. Sustain. Energy*, vol. 5, no. 1, pp. 209–217, Jan. 2014.

[17] M. C. Bozchalui, and R. Sharma, "Operation strategies for energy storage systems in distribution networks," in *Proc. IEEE PES General Meeting,* pp.1-5, Jul. 27-31, 2014.

[18] G. Carpinelli, G. Celli, S. Mocci, F. Mottola, F. Pilo, and D. Proto, "Optimal Integration of Distributed Energy Storage Devices in Smart Grids," *IEEE Trans. Smart Grid*, vol. 4, no. 2, pp.985-995, Jun. 2013

[19] Nick, M.; Hohmann, M.; Cherkaoui, R.; Paolone, M., "On the optimal placement of distributed storage systems for voltage control in active distribution networks," in *Proc. 3rd IEEE PES Int. Conf. Exhibition Innovative Smart Grid Technol.*, 2012, pp. 1–6.

[20] G. Liu, O. Ceylan, Y. Xu, and K. Tomsovic, “Optimal Voltage Regulation for Unbalanced Distribution Networks Considering Distributed Energy Resources,” in *Proc. IEEE PES General Meeting,* pp.1-5, Jul. 26-30, 2015.

[21] G. Liu, Y. Xu, O. Ceylan, and K. Tomsovic, “A new linearization method of unbalanced electrical distribution networks,” in *Proc. 46th North American Power Symposium (NAPS 2014),* Pullman, WA, Sep. 2014.

[22]]T. Saaty, ”Decision making-The analytic hierarchy and network processes (AHP/Anp),” *J. Syst. Sci. Syst. Eng.*, vol. 13, no.1 pp 1-35, Mar. 2004.

[23] G. Liu and K. Tomsovic, "Quantifying spinning reserve in systems with significant wind power penetration," *IEEE Trans. Power Syst.*, vol. 27, no. 4, pp. 2385-2392, Nov. 2012.

[24] Distribution Test Feeders [online] Available: http://ewh.ieee.org/soc/pes/dsacom/testfeeders/.

[25] C. Grigg, P. Wong, P. Albrecht, R. Allan, M. Bhavaraju, R. Billinton, Q. Chen, C. Fong, S. Haddad, S. Kuruganty, W. Li, R. Mukerji, D. Patton, N. Rau, D. Reppen, A. Schneider, M. Shahidehpour, and C. Singh, “The IEEE Reliability Test System-1996. A report prepared by the Reliability Test System Task Force of the Application of Probability Methods Subcommittee,” *IEEE Trans. Power Syst.*, vol. 14, no. 3, pp. 1010-1020, Aug. 1999.

[26] MSX-60 and MSX-64 Photovoltaic Modules. [Online]. Available: https://www.smud.org/en/about-smud/environment/renewable-energy/documents/solar-regatta-photovoltaic-specs.pd

[27] [Online]. Available: http://www.nrel.gov/midc/ornl_rsr/

[28] J. Dupa˘cová, N. Gröwe-Kuska, and W. Römisch, “Scenario reduction in stochastic programming: An approach using probability metrics,” *Math. Program.*, ser. A 95, pp. 493–511, 2003.